

Pulsed Sonoelectrochemical Synthesis of Cadmium Selenide Nanoparticles

Y. Mastai,[†] R. Polsky,[‡] Yu. Kolytyn,[‡] A. Gedanken,^{*,‡} and G. Hodes^{*,†}

Contribution from the Department of Materials and Interfaces, The Weizmann Institute of Science, Rehovot 76100, Israel, and Department of Chemistry, Bar-Ilan University, Ramat-Gan 52900, Israel

Received March 18, 1999

Abstract: Powders of CdSe nanoparticles were prepared by a pulsed sonoelectrochemical technique. The crystal size could be varied from X-ray amorphous up to 9 nm (sphalerite phase) by controlling the various electrodeposition and sonic parameters. The mechanisms for the effects of the various parameters on particle size are discussed. Optical properties of the powders were measured by diffuse reflection spectroscopy and the measured increase in band gap due to size quantization correlated with particle size.

Introduction

Nanoparticles are the subject of considerable interest in many different scientific disciplines. This interest derives from the many special properties of materials in the nanoscale regime, including (photo)catalytic, mechanical, electrical, and optical.^{1–6} Semiconductor nanoparticles in particular exhibit variable and often controllable properties, in particular the change of energy structure (including band gap) and enhanced surface properties with decrease in size which affect all their optoelectronic properties.

Semiconductor nanoparticles have been prepared from many different semiconductors in different forms (colloids, powders, deposited on substrates) and by a variety of methods (ref 7 treats a wide selection of materials and techniques). One of these methods that has been studied by us for some time is electrodeposition to give films of nanocrystals, either isolated or aggregated, on an electrically conducting substrate.^{8–10} We have recently found that the combination of ultrasonic excitation and electrochemical deposition can produce powders of CdSe with a controllable particle size. The size can be controlled over a wider range (toward smaller particles) than using electrodeposition by itself and the high deposition current densities employed allow continuous production of relatively large amounts of the nanopowder.

Sonochemistry has been in use for some time now. It was discovered as early as 1934 that the application of ultrasonic

energy can increase the rate of electrolytic water cleavage.¹¹ The effects of ultrasonic radiation on chemical reactions are due to the very high temperatures and pressures which develop in and around collapsing bubbles (cavitation).¹² However, it is only recently that the potential benefits of combining sonochemistry with electrochemistry have become increasingly studied. Some of these beneficial effects include acceleration of mass transport, cleaning and degassing of the electrode surface, and increased reaction rates.^{13–15} Using a thermostated sonoelectrochemical cell to study homogeneous reactions in solutions, Marken and Compton reported that extremely high limiting currents were detected at significantly negative potentials in the presence of ultrasound.¹⁶ Drake found that, during electrodeposition of Cu, 1.2 MHz and 20 kHz ultrasound reduced the diffusion layer from 200 μm to about 20–30 μm and 3.4 μm , respectively.¹⁷ In addition, the electrodeposition of metals or alloys (e.g., Zn, Cu/Zn, Ni/Fe)^{18,19} and the production of catalytically active powders²⁰ have been reported as a result of combining electrochemistry and ultrasound radiation.

Reisse and co-workers^{20–24} have described a novel device

(11) For early reviews see: Yeager, E.; Hovorka, F. *J. Acoust. Soc. Am.* **1953**, 25, 443. Kaplin, A. A.; Bramin, V. A.; I. E. Stas', I. E. *Zh. Anal. Khim.* **1988**, 43, 921.

(12) Suslick, K. S. *Sci. Am.* **1989**, 260, 80.

(13) Mason, T. J.; Walton, J. P.; Lorimer, D. J. *Ultrasonics* **1990**, 28, 333.

(14) Mason, T. J.; Walton, J. P.; Lorimer, D. J. *Ultrasonics* **1990**, 28, 251.

(15) Mason, T. J. *Practical Sonoelectrochemistry*; Ellis Horwood, Chichester, 1991.

(16) Marken, F.; Compton, R. *Ultrason. Sonochem.* **1996**, S131.

(17) Drake, M. P. *Trans. Inst. Met. Finish.* **1980**, 58, 67.

(18) Mason, T. J. *Chemistry with Ultrasound*; Elsevier: London, 1990.

(19) Kochergin, S. M.; Vyaseleva, G. Y. *Electrodeposition of Metals in Ultrasonic Fields*; Consultants Bureau: New York, 1966.

(20) Reisse, J.; Francois, H.; Vandercammen, J.; Fabre, O.; Kirsch-De Mesmaecker, A.; Maerschalk, C.; Delplancke, J. L. *Electrochim. Acta* **1994**, 39, 37.

(21) Chandlerhenderson, R. R.; Coffey, J. L.; Filesseler, L. A. *J. Electrochem. Soc.* **1994**, 141, L166J.

(22) Durant, A.; Deplancke, J. L.; Winand, R.; Reisse, J. *Tetrahedron Lett.* **1995**, 36, 4257. Reisse, J. *Homogeneous sonochemistry: From physical studies to nanopowder preparation*; presented at the DECHMA annual meeting, Wiesbaden, 1996.

(23) Delpancke J. L.; Dibella V.; Reisse J.; Winand, R. *Mater. Res. Soc. Symp. Proc.* **1995**, 372, 75.

(24) Reisse J.; Caulier T.; Deckerkheer C.; Fabre O.; Vandercammen J.; Delplancke, J. L.; Winand R. *Ultrason. Sonochem.* **1996**, 3, S147.

[†] The Weizmann Institute of Science.

[‡] Bar-Ilan University.

(1) Serpone, N.; Khairutdinov, R. F. In *Semiconductor Nanoclusters, Studies in Surface Science and Catalysis*; Kamat, P. V., Meisel, D., Eds.; Elsevier Science, 1996; Vol. 103, p 417.

(2) Siegel, R. W.; Fougere, G. E. In *Nanophase Materials*; Hadjipanayis, G. C., Siegel, R. W., Eds.; Kluwer Academic Publishers: Hingham, MA, 1994; p 233.

(3) Hagfeldt, A.; Grätzel, M. *Chem. Rev.* **1995**, 95, 49.

(4) Halperin, W. P. *Rev. Mod. Phys.* **1986**, 58, 533.

(5) Sailor, M. J.; Heinrich, J. L.; Lauerhaas, J. M. In *Semiconductor Nanoclusters, Studies in Surface Science and Catalysis*; Kamat, P. V., Meisel, D., Eds.; Elsevier Science: New York, 1996; Vol. 103, p 209.

(6) Weller, H.; Eychmuller, A. *Adv. Photochem.* **1995**, 165.

(7) Chapters in *Nanoparticles in Solid and Solutions*; Fendler, J. H., Dékány, I., Eds.; NATO ASI Series 3; Kluwer Academic Publishers: Hingham, MA, 1996; High Technology, Vol. 18.

(8) Hodes, G. *Isr. J. Chem.* **1993**, 33, 95.

(9) Golan, Y.; Hodes, G.; Rubinstein, I. *J. Phys. Chem.* **1996**, 100, 2220.

(10) Mastai, Y.; Hodes, G. *J. Phys. Chem. B* **1997**, 101, 2685.

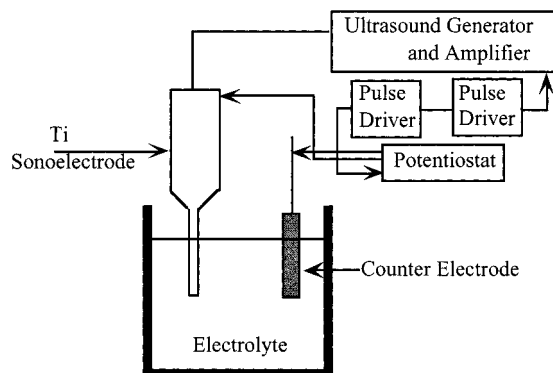


Figure 1. Schematic of the sonoelectrochemical deposition setup.

for the production of metal powders using pulsed sonoelectrochemical reduction. This device exposes only the flat circular area at the end of the sonic tip to the electrodeposition solution. The exposed area acts as both cathode and ultrasound emitter. A pulse of electric current produces a high density of fine metal nuclei. This is immediately followed by a burst of ultrasonic energy that removes the metal particles from the cathode, cleans the surface of the cathode, and replenishes the double layer with metal cations by stirring the solution. Coulomb efficiencies were about 75–90%. The metals were obtained as chemically pure, fine crystalline powders of high surface area with an average particle size of 100 nm. In ref 24, a list of powders prepared by this method, with particle size varying between 10 and 1000 nm depending on deposition conditions, is given. While most are metals or metallic alloys, two nonmetal examples are given, MnO_2 and CdTe ,²⁴ the latter deposited from an aqueous solution of TeO_2 and CdSO_4 . Despite the lack of specific information on these particular samples, the CdTe appears to be the only example up to now of a semiconductor deposited by this technique.

In this work we use a sonoelectrochemical device that is similar to the one described by Reisse and others.^{20–24} While there are several different methods for the electrodeposition of CdSe , we have chosen the one based on the electroreduction of selenosulfate in aqueous solution^{25–27} since it is experimentally the most simple and results in stoichiometric CdSe over a wide range of deposition conditions.

Experimental Section

In Figure 1 we present the schematics of the experimental setup assembled for these experiments. A titanium horn (Ultrasonic liquid processor VC-600, 20 kHz, Sonics&Materials) acts both as the cathode and the ultrasound emitter. The electroactive part of the sonoelectrode is the planar circular surface, of area 1.23 cm^2 , at the bottom of the horn. The immersed cylindrical part is covered by an isolating plastic jacket. This sonoelectrode produces a sonic pulse that is triggered immediately following a current pulse (Figure 2). One pulse driver (General Valve) is used to control a potentiostat and a second one (Wavetek function generator 164) controls the ultrasonic processor, which is adapted to work in the pulse mode (Figure 1). The home-built potentiostat is operated in the constant current regime (without using a reference electrode). A platinum wire spiral (0.5 mm diameter and 15 cm long) is used as a counter electrode. The current pulses were $0.25 \text{ A}\cdot\text{cm}^{-2}$. The duration of the current pulse was 0.34 s unless otherwise stated. The off time of the current pulse was always 0.34 s, the same as the duration of the ultrasonic pulse. Prior to electrodepo-

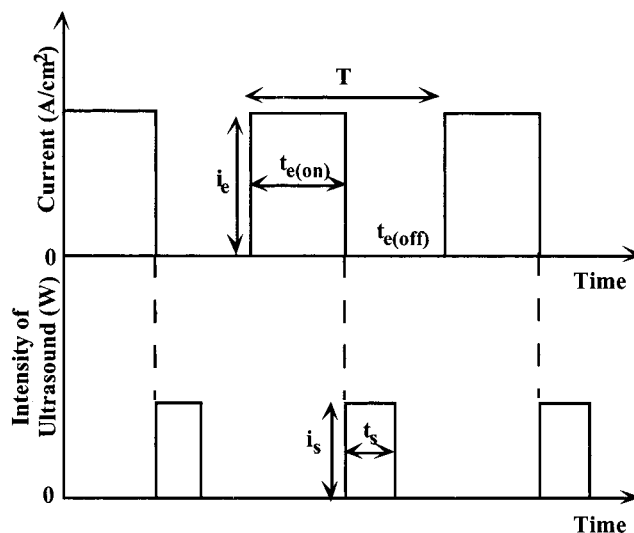


Figure 2. Schematic of the sonic and electrochemical waveforms.

sition, the sonoelectrode was sonicated in 50:50 acetone–distilled water solution for 5 min at an ultrasound intensity of 50 W. The ultrasound pulse intensity was varied up to $60 \text{ W}\cdot\text{cm}^{-2}$ with a duration (t_s) of 0.34 s. Some experiments in which continuous, rather than pulsed, ultrasonic excitation was employed were also carried out.

The electrolyte was based on that used by Cocivera et al.²⁶ An aqueous solution of CdSO_4 , complexed with potassium nitrilotriacetate ($\text{N}(\text{CH}_2\text{CO}_2\text{K})_3 = \text{NTA}$) was mixed with an aqueous sodium selenosulfate solution (Na_2SeSO_3) to give a final concentration of 80 mM each CdSO_4 and Na_2SeSO_3 and 160 mM NTA at a pH between 8 and 10. The exact composition of the electrolyte is not critical, but it is important that the solution pH is greater than 7 before addition of Na_2SeSO_3 (to prevent formation of free Se) and that the $\text{CdSO}_4:\text{N}(\text{CH}_2\text{CO}_2\text{K})_3$ ratio and pH are low enough to prevent chemical solution deposition of CdSe (refs 28 and 29 explain the interplay of these factors in the chemical deposition reaction). The electrolyte volume ranged from 50 to 200 mL. The deposition was carried out for typically 30 min. At the end of the reaction, the precipitate was centrifuged, washed repeatedly with acetone, and dried under vacuum.

Characterization Methods

Optical Spectra. Diffuse Reflection Spectroscopy (DRS) measurements were carried out on a Jasco V-570 spectrophotometer equipped with an integrating sphere. Spectra were recorded at room temperature, from 1000 to 400 nm with a scanning speed of 100 nm/min. MgCO_3 was used as a reference. Bulk powder of CdSe was used as a comparison. The spectra are given as plots of the Kubelka–Munk remission function^{30,31} (converted from the diffuse reflectance values by the spectrophotometer software) vs wavelength. These plots correspond fairly well to absorption spectra.

X-ray Diffraction. Powder X-ray diffraction (XRD) spectra of the powders were obtained using a Rigaku RU-200 B Rotaflex diffractometer operating in the Bragg configuration using $\text{Cu K}\alpha$ radiation. Data were collected with a counting rate of $0.25 \text{ deg min}^{-1}$ and sampling interval of 0.002° . The accelerating voltage was set at 50 kV with a 150 mA flux. Scatter and diffraction slits of 0.3 and 0.5 mm collection slits were used. The crystal size (coherence length) was estimated from the width of the diffraction peaks using the Debye–Scherrer relationship.

Transmission Electron Microscopy (TEM). A Phillips EM-400T electron microscopy operating at 100 kV was used for TEM and electron diffraction (ED).

(25) Skyllas-Kazacos, M.; Müller, B. *J. Electrochem. Soc.* **1980**, *127*, 2378.

(26) Cocivera, M.; Darkowski, A.; Love, B. *J. Electrochem. Soc.* **1984**, *131*, 2514.

(27) Szabo J. P.; Cocivera, M. *Can. J. Chem.* **1988**, *66*, 1065.

(28) Gorer, S.; Hodes, G. *J. Phys. Chem.* **1994**, *98*, 5338.

(29) Gorer, S.; Hodes, G. In *Semiconductor Nanoclusters: Physical, Chemical and Catalytic Aspects*; Kamat, P. V., Meisel, D., Eds.; Elsevier Scientific, 1997; p 297.

(30) Kubelka, D.; Munk, L. *J. Opt. Soc. Am.* **1948**, *38*, 448.

(31) Kortüm, G. *Reflectance Spectroscopy*; Springer: Berlin, 1973.

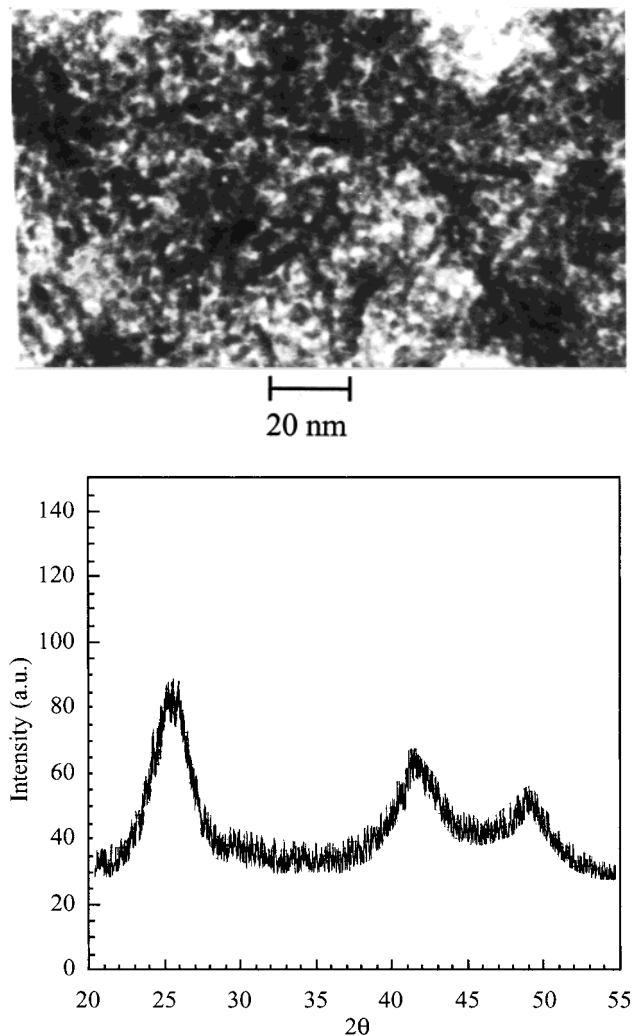


Figure 3. (a) TEM image of a CdSe powder (sample B in Table 1). (b) XRD spectrum of sample B.

Coulter Counter. Mean particle size distribution was determined by dynamic light scattering of the suspension of the particles in aqueous solution with a Coulter N-4 particle size analyzer.

Results

There are many experimental variables involved in sonoelectrochemical deposition: electrolyte composition and temperature; electrodeposition conditions including current density, pulse on time, and ratio between pulse on time and off time (duty cycle); and sonic probe conditions (power, pulse parameters). While we have not made an exhaustive investigation of the effects of all these parameters on the properties (and particularly on the crystal size) of the deposited CdSe, we have studied a range of deposition conditions.

First we show a TEM micrograph (Figure 3a) and XRD spectrum (Figure 3b) of a typical powder formed by the sonoelectrochemical method to demonstrate the ability of this technique to prepare nanocrystalline powders. The particles were either spherical or slightly oblate. The average size estimated from both TEM and XRD is 4.0 nm. The XRD spectrum is characteristic of sphalerite (cubic) CdSe.

Table 1 sums up the effects of some of the experimental variables on crystal size and CdSe band gap (the latter to be discussed below). In general, decreasing temperature, shorter pulse duration, and higher sonic intensity all lead to a decrease in crystal size. With the exception of sonic intensity in the low-

intensity region, which has a major effect on crystal size, the effects of these variables on crystal size, while not very large, are appreciable. They are particularly important since the crystal sizes vary in the strong size quantization regime where even a modest change in crystal size can result in a large change in optoelectronic properties.³²

Size distribution histograms, measured directly from TEM micrographs, of some of the samples shown in Table 1 are given in Figure 4. The average sizes calculated from these histograms, together with those estimated from the corresponding XRD spectra using the Debye–Scherrer analysis and the standard deviation calculated from the histograms, are also shown.

To separate the effects of the sonic excitation from those of pulse electrodeposition, we briefly compare the differences between CdSe films prepared on SnO₂ conducting glass using both pulsed and continuous electrodeposition in the absence of sonic excitation. The comparison is limited since the high current density used for the pulse deposition cannot be maintained in continuous deposition (depletion effects would seriously affect the layer). The (lower current density, 1 mA·cm⁻²) continuous deposited CdSe is made up of substantially larger crystals (20–30 nm), measured by TEM, than the pulse-deposited CdSe (ca. 9 nm). It should be mentioned that the XRD spectrum of the continuous deposited CdSe is very broad: assuming crystal size broadening, the crystal size would be no more than 4 nm. The TEM measurements show that the crystals are much larger than this, therefore the XRD broadening in this case is presumed due to defects in the crystals (faults, strain).³³ We have previously explained the unusual shape of the absorption spectrum of CdSe films electrodeposited from these solutions (continuous current and without sonic excitation) as arising from strain in the crystals.³⁴ The nontrivial relationship between the broad XRD peak widths measured by us and others for these films and crystal size (and size-dependent properties) have been discussed in more depth.³⁵ We note that for almost all cases of small nanocrystals (<10 nm) which we have studied, the XRD and TEM estimations of size are comparable. The effect of pulsed electrodeposition on the crystal size of semiconductors will be the subject of a separate study.

Samples were also prepared by pulse plating with a continuous sonic wave. The powders prepared under these conditions were found to be XRD amorphous and their electron diffraction pattern consisted of a very broad ring.

The plating current density was found to be an important factor in determining crystal size. Lower current density (for the same time) resulted in larger crystal size (ca. 10 nm at 0.1 A·cm⁻²) compared with 5 nm at 0.25 A·cm⁻². We were unable, at this time, to use higher current densities, but it is reasonable to expect that even smaller crystals might be obtained under such conditions.

Finally, we chose a combination of parameters to obtain a particularly small crystal size. This is shown by sample A in Table 1. CdCl₂ was chosen instead of CdSO₄ since chloride ion is more strongly adsorbing than sulfate and was therefore more likely to block crystal growth, as has been seen in CdS and CdSe deposition from organic electrolytes.⁸ While the CdCl₂ by itself had only a marginal effect on crystal size, the

(32) Murray, C. B.; Norris, J.; Bawendi, M. G. *J. Am. Chem. Soc.* **1993**, *115*, 8706.

(33) Guinier, A. In *X-ray Diffraction*; W. H. Freeman and Company: New York, 1963.

(34) Hodes, G.; Albu-Yaron, A.; Decker, F.; Motisuke, P. *Phys. Rev. B* **1987**, *36*, 4215.

(35) Hodes, G. In *Physical Electrochemistry: Principles, Methods, and Applications*; Rubinstein, I., Ed.; Marcel Dekker Inc.: New York, 1995; p 529.

Table 1. Effect of Various Deposition Parameters on CdSe Properties

variable parameter	sample conditions	XRD size (nm)	TEM size (nm)	E_g (eV)	E_g calcd from size ^{c,32}
temp	5 °C	4	4.5	2.10	2.15
	Sample C: 25 °C	5	5.5	≈2.1	2.05
	75 °C	6.5	6.5	1.93	1.98
ultrasound intensity	0 W ^b	9	8.5	1.81	1.90
	10 W	10	10	1.70	1.85
	30 W	5	5	2.00	2.06
	60 W	4	4.5	2.10	2.15
current pulse width (off time 0.34 s)	Sample D: 0.68 s	7	8	1.73	1.95
	0.34 s	5	5.5	1.90	2.05
	0.11 s	4	4.5	2.10	2.15
miscellaneous	Sample B	4	4	2.14	2.20
	CdCl ₂ (current pulse width 0.11 s)				
	Sample E continuous ultrasound	amorphous		2.07	
	Sample A CdCl ₂ (5 °C, 60 W, current pulse width 0.11 s) no sonic, DC plating ^b	3.5	3	2.16	2.35
		N/A	20–30 ³⁴	1.71 ³⁴	1.80 (bulk)

^a Standard conditions, unless given otherwise, are as follows: $T = 25$ °C; current density = $250 \text{ mA}\cdot\text{cm}^{-2}$; current pulse width = 0.34 s; current off time = 0.34 s; ultrasound intensity = 20 W. ^b Thin film deposited on SnO₂. ^c The expected band gap based on the measured crystal size and using the size–band gap correlations from ref 32.

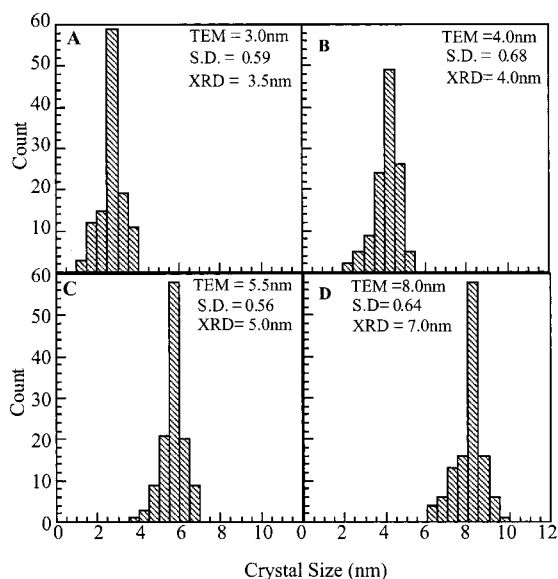


Figure 4. Crystal size distributions of four different nanocrystalline powders of CdSe prepared under different conditions (labels identify samples from Table 1). Since the particles were often slightly oblate, an average size between the two in-plane dimensions was used to estimate the size of each particle.

combination with low temperature, high ultrasonic power, and short deposition pulse resulted in the smallest crystal size obtained by us, 3.5 nm.

The importance of controlling crystal size in the quantum dot size regime (for CdSe, smaller than 12 nm) is expressed in the variation of the semiconductor energy level structure, and therefore optoelectronic properties, with crystal size. Of these properties, optical transmission (absorption) spectra are often the most commonly and simply measured. We note that the color of the powders varied from brown (for the largest crystal sizes) to orange-red (sample A in Table 1). For this reason, it was important to correlate the different crystal sizes prepared here with their optical spectra. Since our product was a powder, we employed diffuse reflection (DR) spectroscopy as a characterization tool. The optical band gap, E_g , was estimated from the DR spectra on the basis of the expected similarity between the Kubelka–Munk (KM) corrected spectra, shown in Figure

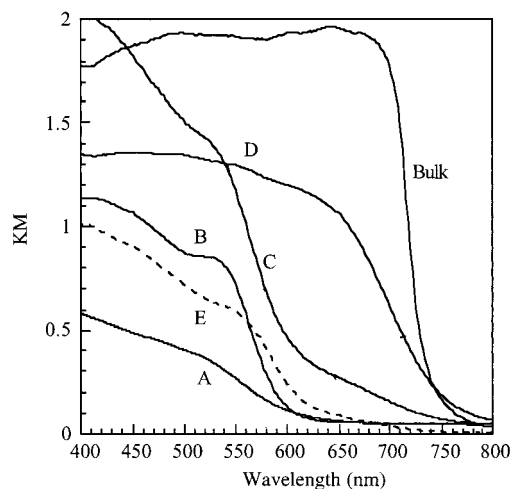


Figure 5. Plot of Kubelka–Munk remission functions (from diffuse reflectance spectra) for different nanocrystalline powders of CdSe. Labels identify samples from Table 1. “Bulk” refers to a bulk (commercial) powdered sample. The absolute values of the KM function are not important here, since they are a function of, among other factors, the amount of material sampled. The spectral shapes contain the relevant information. Note that the broad onset tail in spectrum C is not considered in analyzing this spectrum, but rather the sharp onset at ca. 600 nm. This tail could conceivably be due to the size distribution, although it is not clear why it should be greater here than in other samples with comparable size distributions.

5, with absorption spectra of films of the same material.³¹ E_g was estimated to correspond to the wavelength ca. one-third up the main absorption feature. We have found this to be a good approximation for quantized semiconductor films as long as their spectral shape behaves like that of a direct band gap semiconductor.⁸ While the spectral shapes of these samples are not always ideally characteristic of a direct band gap semiconductor, this approximation is used here. For other reasons, the band gap estimates are only approximate. These include the size distribution of the crystals (which will smear out the spectra), the gradual onset of some of the spectra (particularly noticeable in spectrum C), and the fact that the KM value has been reported to depend on the particle size.³¹

While the CdSe described above was obtained as a precipi-

tated powder, colloidal solutions of CdSe could also be prepared. For this purpose, a capping agent that prevents aggregation in the strong electrolyte is necessary. We used sodium polyphosphate and measured the aggregate size using a Coulter counter. In the absence of the polyphosphate, the CdSe readily precipitates and the aggregate size is greater than that measurable by the counter (3500 nm). The aggregate size decreases with increasing amount of polyphosphate, from 3000 nm for 0.1 M to 200 nm for saturated polyphosphate (ca. 0.4 M). For the latter, while precipitation did occur, it was much slower (the solution remained colored for about an hour after sonication) compared with the almost immediate precipitation of the CdSe in the absence of polyphosphate. Interestingly, after reaching a maximum aggregate size in some tens of minutes under the conditions used by us, the aggregate size decreased with increasing time, particularly for the larger aggregates. This is probably due to gradual breakup of the aggregates by the sonoprobe. While we did not investigate this effect further, it is probable that the aggregate size and therefore colloidal stability can also be controlled by the sonic intensity. The use of more effective capping agents, such as phosphine and phosphine oxides (tri-*n*-butylphosphine, tri-*n*-octylphosphine oxide [TOPO]),^{10,32} should also contribute to more stable colloidal solutions.

Discussion

The basis of the sonoelectrochemical technique to form nanoparticles is massive nucleation using a high current density electrodeposition pulse (250 mA·cm² in this work), followed by removal of the deposit from the sonoelectrode by the sonic pulse. Removal of the CdSe from the electrode before the next current pulse prevents crystal growth. The effects of the various parameters on crystal size can be rationalized as follows.

Temperature. Temperature can affect crystal growth in several ways, all of them resulting in smaller crystal size at lower temperatures. The simplest is that crystal growth is slower at lower temperatures. Within the time between sonic pulses, growth can occur, either by coalescence during the deposition pulse or by migration on the substrate and coalescence at any time. Also, if the sonic pulse does not completely remove the deposit (a likely occurrence since the crystal size is dependent on the sonic pulse intensity), there is even more opportunity for the crystals on the substrate to grow. In addition, the crystals, particularly the smaller ones, might also grow to some extent by coalescence in the electrolyte after removal from the electrode.

Another effect of temperature is through the thermodynamic instability of very small nuclei below a certain critical size. These nuclei should redissolve, but may be stable for long enough to grow larger than the critical size, after which they are thermodynamically stable. This kinetic stabilization will be more effective at lower temperatures. This is a common mechanism to explain the decrease in colloid size with decrease in temperature. It may be operative also here, although the presence of the heterogeneous substrate (the electrode) can also exert an additional stabilizing influence on nuclei which would be sub-critical in the absence of this surface.

Sonic Intensity. As implied above, the greater the sonic intensity, the greater will be the efficiency of removal of the deposit and therefore the less chance there will be for crystal growth of existing nuclei. Above a certain intensity where all the deposit is removed, further increase in intensity is not expected to affect growth much (there may be some effect inasmuch as growth can occur during the sonic pulse before all the deposit is removed and the greater the sonic power, the

faster will be the deposit removal). It appears that we have not yet reached this intensity, since crystal size decreased up to our maximum intensity (60 W). Note that in the absence of sonic excitation, the CdSe forms as a film on the electrode. To be able to measure the optical properties of this film, the substrate used was transparent conducting glass.

Deposition Current Pulse Width. Quite separately from the sonic wave effects, pulse electrodeposition is well-known to result in a smaller crystal sized deposit.^{36,37} This is particularly pronounced for high current densities (high overpotentials), where a high rate of nucleation occurs during each pulse. The shorter the pulse duration, the less chance there is of crystal growth occurring by deposition of new material on a previous nucleus. In normal pulse plating, crystal size may or may not increase with the number of pulses, depending on whether each new pulse forms a new nucleus or adds to preexisting ones. In sonoelectrochemical deposition, where the deposit is (to a greater or lesser extent) removed during each sonic pulse, only new nuclei should be formed, and therefore the crystal size will be smaller still.

The change in band gap of CdSe as a function of crystal size has been treated both theoretically and experimentally by many groups. We have used the optical absorption data for the wurtzite (hexagonal) CdSe quantum dots of Murray et al.³² to estimate the band gap/crystal size correlation. Since our quantum dots are sphalerite CdSe, with a slightly higher band gap (ca. 1.8 eV³⁸) than that of wurtzite CdSe (1.73 eV), we have added 0.07 eV (the difference between these two values) to the band gaps for the hexagonal CdSe obtained from the data of Murray et al. The dependence of band gap with size is expected to be very much the same for the two crystal forms since the effective masses for the two forms, which are the main determining factor for this dependence, are almost identical.³⁸ These values are given in the last column of Table 1.

In general, the values of E_g estimated from the DR spectra are lower than those expected based on measured size. The discrepancy is more noticeable for the smaller crystal sizes. While the method of band gap measurement used by us is an approximation, it is certainly not as inaccurate as to lead to the difference of almost 0.2 eV seen between the measured and expected band gaps of the smallest crystal-size sample (A). It may be that the individual crystallites in the powders are aggregated in a way that there is moderate electrical conductivity between them, thus reducing the degree of size quantization. Increased coalescence of metallic nanoparticles has been shown to occur in ultrasonic reactions.³⁹ This is in contrast to chemically deposited films composed of aggregated quantum dots, where the aggregation does not appear to affect the degree of quantization (i.e., the value of E_g corresponds closely to that expected based on quantum dot size⁸). Another factor that would lead to some underestimation of the band gap values from the optical spectra is the likelihood that the onset of the absorption spectra are dominated by crystals in the distribution somewhat larger than the average crystal size. However, it is clear from Table 1 that there is an overall correlation between smaller crystal size and larger band gap.

Concerning the amorphous CdSe obtained using constant sonic excitation, it is known that sonochemical preparation of

(36) Choo, R. T. C.; Toguri, J. M.; El-Sherik, A. M.; Erb, U. *J. Appl. Electrochem.* **1995**, *25*, 384.

(37) McMahon, G.; Erb, U. *J. Mater. Sci. Lett.* **1989**, *8*, 865.

(38) *Landolt-Börnstein*; Madelung, O., Ed.; Springer-Verlag: Berlin-Heidelberg-New York, 1982; Vol. III/17b.

(39) Doktycz, S. J.; Suslick, K. S. *Science* **1990**, *247*, 1067.

metals often results in amorphous materials^{40–42} due to rapid cooling of the local high temperatures in the cavitation bubbles. There is no reason to expect that the electrodeposited CdSe will be enclosed in the cavitation bubbles. A more likely explanation for the “amorphous” formation is that the CdSe does not have an opportunity to grow to a size that is detectable by XRD (typically >2 nm).

A larger crystal size was obtained at lower plating current densities (10 nm at 0.1 A·cm⁻² vs 5 nm at 0.25 A·cm⁻²). Current density can affect crystal size in at least two opposing directions. A smaller size would be expected based on the smaller amount of material deposited at lower currents. On the other hand, lower currents (per unit time) allow more time for atomic diffusion processes to occur which can lead to larger crystal size. In the absence of other effects, it seems that the latter is dominant in this case.

The measured band gap of the amorphous CdSe (2.06 eV) is considerably higher than that for crystalline CdSe but smaller than what would be expected if the powder was composed of <2 nm size-quantized crystals. The band gaps of amorphous semiconductors may be either higher or lower than those of the corresponding crystalline material. We have shown that CdSe, electrodeposited from a solution of Cd(ClO₄)₂ and Se in

DMSO onto Pd substrates, contains CdSe “crystallites” of ca. 1 nm in size surrounded by disordered (amorphous) CdSe.⁴³ Using photocurrent spectroscopy, the band gap of this close-to-amorphous CdSe was observed to be very similar to that of normal crystalline CdSe.⁴⁴ It may be that the XRD amorphous CdSe prepared by constant sonic excitation is similar, but with a higher fraction of crystalline material. The gradual long wavelength onset would then be characteristic of the amorphous component while the apparent band gap onset, at ca. 2.06 eV, would arise from very tiny nanocrystals which, because of the surrounding amorphous material, only exhibit partial size quantization.

In conclusion, we have demonstrated a sonoelectrochemical method for preparation of nanopowders of semiconductors where the nanoparticle size can be controlled using a wide range of deposition parameters. This technique should be applicable to other materials which can be electrodeposited and easily scaleable for large-quantity preparation.

Acknowledgment. This work was supported by the Israel Ministry of Science, Contract Nos. 5839-2-96 and 8461-1-98 (to G.H.), and by a NEDO International Joint Research Grant (to A.G.).

(40) Suslick, K. S.; Choe, S. B.; Cichovlas, A. A.; Grinstaff, M. W. *Nature* **1991**, 353, 414.

(41) Cao, X.; Prozorov, R.; Kolytyn, Yu.; Katabi, G.; Gedanken, A. *J. Mater. Res.* **1997**, 12, 402.

(42) Haasen, P.; Jaffee, R. I. *Amorphous Metals and Semiconductors*; Pergamon: London, 1984.

JA9908772

(43) Golan, Y.; Ter-Ovanesyan, E.; Manassen, Y.; Margulis, L.; Hodes, G.; Rubinstein, I.; Bithell, E. G.; Hutchison, J. L. *Surf. Sci.* **1996**, 350, 277.

(44) Alpers, B.; Rubinstein, I.; Hodes, G. Unpublished results